Viser Technology Pte. Ltd.
Mechanical Engineering Science
DOI: 10.33142/mes.v5i2.12717

Research Article Open Access

Effects of Material Parameters on Stress Distribution in Casing-cement -formation (CCF) Multilayer Composite System

Chao ZHANG[1], Yuanbo XIA[2, 3], Bo ZHOU[1*], Xiuxing ZHU[1], Haijing WANG[1]

1. College of Pipeline and Civil Engineering, China University of Petroleum (East China), Qingdao, Shandong, 266580, China
2. School of Petroleum Engineering, China University of Petroleum (East China), Qingdao, Shandong, 266580, China
3. CNPC Tianjin Bo-Xing Engineering Science &Technology Co., Ltd., Tianjin, 300451, China

*Corresponding Author: Bo ZHOU, E-mail: zhoubo@upc.edu.cn

Abstract

This work focus on the stress distribution of the casing-cement -formation (CCF) multilayer composite system, which is a borehole system with multiple casings and cement sheathes. Most of the previous relevant studies are based on the traditional CCF system with the single casing and cement sheath, but these results are not adaptive to the CCF system multiple composite system. In this paper, the FEM numerical model of CCF multilayer composite system was constructed. Numerical simulations were calculated and compared with the system which consists of the single casing and cement sheath. Results show that the multilayer composite system possesses better performance. On this basis, the sensitivity analysis of main influence mechanical parameters such as in-situ stress, the elastic of cement sheathes and the elastic of formation are conducted. The cement sheath on the inside, namely cement sheath-1, is sensitive to its elastic modulus; meanwhile, the cement sheath on the outside, namely cement sheath-2, is not so sensitive to the elastic modulus of cement sheath-1. Cement sheath-1 and cement sheath-2 are all sensitive to the elastic modulus of cement sheath-2, and the mises stress of them has opposite trend to the elastic modulus of cement sheath-2. The proper values of elastic modulus of cement sheath-1 and cement sheath-2 are 5GPa and 5GPa to 30GPa, respectively. Under the in-situ stress ratio σh / σH = 0.7, the maximum mises stress of cement sheath-1 and cement sheath-2 increase as the increase of σh, and they are nearly equal when σh=15GPa. This research can be helpful for the design and analysis of CCF multilayer composite system.

Keywords: *In-situ stress; Stress distribution; Casing; Cement sheath; Formation; Multilayer*

1 Introduction

Casing-cement-formation (CCF) system is the borehole system commonly used for oil and gas exploitation operations in the petroleum industry [1-3]. This system is integral to maintaining borehole stability, ensuring the efficient production of hydrocarbons and providing a critical barrier against the uncontrolled flow of fluids between subsurface formations. However, when the system is subjected to the in-situ stress and internal pressure of drilling fluid, the mechanical integrity, especially the cement sheath, is often damaged. Then the formation fluid migrates from cracks and leading to the failure of annulus sealing [4-5]. Therefore, the research on the stress field of the CCF system is crucial to petroleum engineering.

The analytical method is one of the main methods to obtain the stress distribution of cement sheathes and casings. Yin et al. [6-7] formulated the analytical elastic solutions for a borehole system with the single of casing and cement sheath under the uniform and non-uniform in-situ stress, respectively. Besides the elastic analysis, Zhang et al. [8] derived the elastoplastic solutions of cement sheath under varied casing pressure. Considering the anisotropy of formation, Wang et al. [9-10] derived analytical solutions for cased borehole stress calculation in general anisotropic formations, which is closer to reality. In view of the far-field displacement boundary of the model of CCF is mostly not fixed, Yu et al. [11] proposed a modified model with a fixed far-field displacement boundary condition. In addition, considering the complexity of analytical solutions, Zhou et al. [12] proposed a semi-analytical method, it should be noticed that this method can not only simplify the calculation but also applicable for the borehole with multiple casings and cement sheathes.

In order to get the experimental data, many scholars conducted mechanical experiments about CCF system [13-15]. Bu et al. [16] designed a device for testing the interface radial bond strength, whose test results can be helpful to study the sealing integrity of cement sheath. Wu et al. [17] employed the digital image correlation (DIC) technique to examine the strain distribution and failure of cement sheath. Li et al. [18] studied the failures of ordinary cement sheath and expanding cement sheath through indoor experiments. Yan et al. [19] conducted a perforating

Received on November 3, 2023; Accepted on December 15, 2023

experiment in real size to investigate the damage mechanism of cement sheath. With the development of computer technology, many numerical methods have been favored by scholars which overcome the limit of the expensive experimental costs and the intricacy of analytical method. Fortunately, there are some available numerical methods to solve the practical problems, such as finite difference method (FDM) [20], finite element method (FEM) [21-22], boundary element method (BEM) [23], meshless methods [24] and so on.

The mentioned above just concentrated on the CCF system with the single casing and cement sheath. As the appearance of deep wells and ultra-deep wells [25-27], the operational environments and conditions becoming more complex, which is a greater challenge to the integrity of the CCF system. The CCF composite system which consists of multiple casings and cement sheathes is an efficient structure in deep wells and ultra-deep wells [28-29]. As for the existing researches for CCF multilayer composite systems, Zhou et al. [12] proposed the semi-analytical method which can conveniently obtain the stress distribution on every casing and cement sheath; based on the relevant theories of heat transfer and elastoplastic mechanics, Li et al. [33] formulated the thermal stress field of CCF multilayer composite systems; Huang et al. [34] conducted the application of hydra-jet fracturing technology in CCF with three layers casings, which provide the detailed references to simulate such well as with multi-layer casings.

However, most of the previous studies are based on the traditional CCF system with the single casing and cement sheath, which are not adaptive to the CCF multiple composite system. In this paper, the numerical model is constructed, which can be used for the comprehensive analyses of CCF multilayer composite system, and the stress fields of casings, cement sheathes and formation are calculated. A series of sensitivity analysis of main parameters are carried out, the results are valuable and helpful to design the CCF multilayer composite system. The rest of this paper is as follows: Firstly, the theoretical analysis of CCF multilayer composite system is elaborated in Section 2. Secondly, the basic theory of FEM correlation is stated in Section 3. Next, the FEM numerical model of CCF multilayer composite system is constructed and the comprehensive analyses of stress field are conducted in Section 4. Finally, this work is summarized, and some conclusions are concluded in Section 5.

2 Mechanical Analysis of CCF Multilayer Composite System

Figure 1 shows a casing-cement-formation (CCF) multilayer composite system, which subjected to the non-uniform in-situ stress. The CCF multilayer composite system can be seemed as a multilayer thick-walled cylinder, in which the inner pressure of the innermost casing, p_w, is induced by drilling fluid. The inner radius of the innermost casing is denoted by r_0, and the outer radius of other casings and cement sheathes are denoted by r_i (i = 1, 2, …, n) in sequence. From the innermost layer, the elastic modulus and Poisson's ratios of the casings and cement sheathes are denoted by E_i (i = 1, 2, …, n) and μ_i (i = 1, 2, …, n) in sequence, respectively. And the elastic modulus and Poisson's ratios of the formation are denoted by E_{n+1} and μ_{n+1}, respectively.

In this section, the model of the casing-cement-formation multilayer composite system is simplified to a plane strain problem, and the following assumptions are satisfied: (1) the casings, cement sheathes and formation are uniform and isotropic linear elastic materials; (2) the casings, cement sheathes and borehole are concentric; (3) the bonding surface between casings, cement sheathes and formation are completely consolidated.

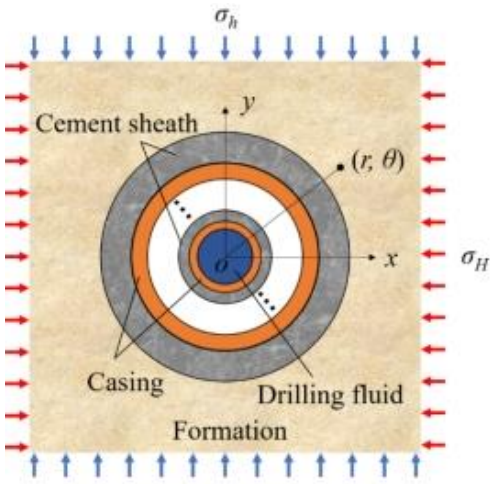

Figure 1 Diagram of CCF multilayer composite system, where σ_H is the maximum horizontal in-situ stress, and σ_h is the minimum horizontal in-situ stress

According to coordinate transformation in the elasticity theory [30], the in-situ stress shown in Figure 1 can be decomposed into the spherical stress tensor read as Eq. (1) and the deviatoric stress tensor read as Eq. (2).

After the decomposition of non-uniform in-situ stress shown in Figure 2, the initial problem can be transferred as the sum of two subproblems, one is the uniform load problem that the CCF multilayer composite system subjected to the inner pressure of drilling fluid and uniform stress shown in Eq. (2); the other is the system subjected to the deviatoric stress shown in Eq. (1). According to the superposition principle [7], the stress field of the CCF multilayer composite system, shown in Figure 1, should be the sum of the uniform stress field formulated by Eq. (3) and the deviatoric stress field formulated by Eq. (4), then the stress field of CCF multilayer composite system can be obtained.

$$s = \frac{1}{2}(\sigma_H - \sigma_h) \tag{1}$$

$$\sigma = \frac{1}{2}(\sigma_H + \sigma_h) \tag{2}$$

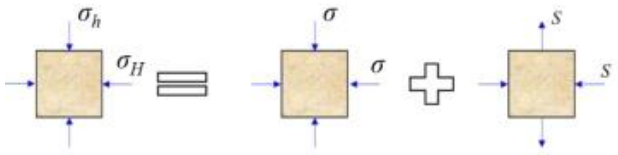

Figure 2 Decomposition of in-situ stress tensor, where (a) is the in-situ stress tensor, (b) is the spherical stress tensor, (c) is the deviatoric stress tensor

According to the reference [31], the solution of the subproblem of uniform load is as

$$a_i P_{i+1} - b_i P_i + c_i P_{i-1} = 0, (i = 1, \ldots, n-1) \tag{3}$$

where a_i, b_i and c_i are coefficients related to geometric and material parameters of casings, cement sheathes and formation; P_i is contact pressure of the contact surface between casings, cement sheathes and formation. When i=1, $P_{i-1}=P_w$; when i=n-1, $P_{i+1}=\sigma$. Based on the Eq. (3), an equation set with n-1 unknows about $P_1 \sim P_n$ can be obtained, thus the contact pressure of each contact surface can be solved. Then the stress distribution of casings and cement sheathes can be obtained by substituting the contact pressure into the Lamey's formula [30],

$$\left.\begin{aligned} \sigma_r &= -\frac{\frac{r^2}{r_2^2}-1}{\frac{r^2}{r_1^2}-1} q_1 - \frac{1-\frac{r^2}{r_1^2}}{1-\frac{r^2}{r_2^2}} q_2 \\ \sigma_\theta &= \frac{\frac{r^2}{r_2^2}+1}{\frac{r^2}{r_1^2}-1} q_1 - \frac{1+\frac{r^2}{r_1^2}}{1-\frac{r^2}{r_2^2}} q_2 \end{aligned}\right\} \tag{4}$$

where r_2 represents the outer radius; r_1 represents the inner radius; q_1 represents the inner pressure; q_2 represents the outer pressure.

For the subproblem of cosine load, the stress distribution of each contact interface is as

$$\left.\begin{aligned} (\sigma_r)_i &= -(2B_i + 4C_i r^{-2} + 6F_i r^{-4}) \cos 2\theta \\ (\sigma_\theta)_i &= (12A_i r^2 + 2B_i + 6F_i r^{-4}) \cos 2\theta \\ (\tau_{r\theta})_i &= (6A_i r^2 + 2B_i - 2C_i r^{-2} - 6F_i r^{-4}) \sin 2\theta \end{aligned}\right\} \tag{5}$$

where A_i, B_i, C_i, F_i are coefficients related to the geometric and material parameters of casings, cement sheathes and formation. Using displacement and stress continuity conditions and stress boundary conditions, the undetermined coefficients in Eq. (5) casings, cements and formation can be obtained.

3 FEM Basically Principle

The FEM is an efficient numerical method to find approximated solutions of the field variables in the problem domain. According to the FEM theory, the problem domain is firstly divided into several elements, as shown in Figure 3, and the connecting points between the elements are called nodes; then the field variables to be seek are set as the interpolation function of nodes; based on the variational principle, the problem can be transformed into a system of algebraic equations where the field variables of all nodes are unknown; finally, the boundary conditions are used to solve the system of algebraic, and the approximate solution of the field variables are obtained subsequently.

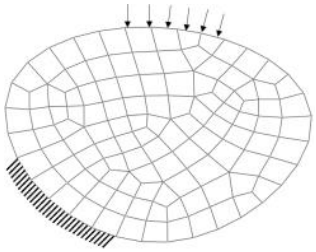

Figure 3 A FEM discrete structure of two-dimensional elasticity problem, which includes nodes and elements

For the two-dimension elasticity domain, the unknown field variable is displacement component. The displacement of a random point c in the domain shown in Figure 4 can be expressed as

$$u(\mathbf{x}) = \mathbf{p}^{\mathrm{T}}(\mathbf{x})\mathbf{b} \tag{6}$$

where P(x) is the vector polynomial basis functions, whose number of monomials can vary from 3 to 10, as listed in Tab. 1; b is the vector of undetermined coefficients related to polynomial basis functions.

$$\mathbf{b} = \left[b_1,\ b_2,\ \cdots,\ b_m\right]^{\mathrm{T}} \tag{6.1}$$

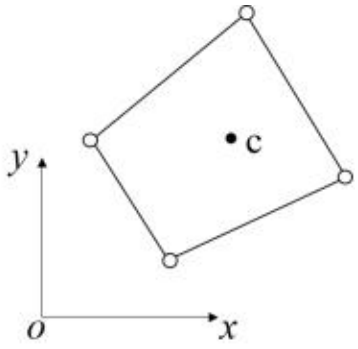

Figure 4 The random point c in the element

Table 1 The vectors of polynomial basis functions for two-dimensional domains, where m is the number of monomials [32]

m	p(x)
3	$[1, x, y]^T$
4	$[1, x, y, xy]^T$
5	$[1, x, y, x^2, y^2]^T$
6	$[1, x, y, x^2, xy, y^2]^T$
7	$[1, x, y, x^2, y^2, x^3, y^3]^T$
8	$[1, x, y, x^2, xy, y^2, x^3, y^3]^T$
9	$[1, x, y, x^2, y^2, x^3, x^2y, xy^2, y^3]^T$
10	$[1, x, y, x^2, xy, y^2, x^3, x^2y, xy^2, y^3]^T$

Therefore, the displacement components of the point c shown in Figure 4 can be represented by that of the nodes on the element. So the displacement function can be expressed as

$$u(\mathbf{x}) = \mathbf{N}\mathbf{a}_e = \sum_{i=1}^{n} N_i u_i \tag{7}$$

where N is the vector of shape functions, N_i is the shape function related to node I; u_i is the nodal displacement.

Substituting the displacement function into the geometric function, we can obtain the element strain matrix. Further, the element stiffness matrix K_i is obtained according to the variational principle [32].

The relationship between nodal displacements and equivalent loads is expressed as

$$Ka=P \tag{8}$$

where K is the global stiffness matrix; P is the global vector of nodal equivalent loads; a is the global vector of nodal displacements, read as

$$\mathbf{a} = [u_1, v_1, u_2, v_2, \ldots, u_M, v_M]^{\mathrm{T}} \tag{9}$$

M is the total number of nodes in the discrete structure shown in Figure 3. Solving the Eq. (8) can we obtain the value of total nodal displacement components. Then the nodal stress and strain components can be obtained by substituting the above values into the geometric function and physical function [32]. The global stiffness matrix is formulated as

$$\mathbf{K} = \sum_{i=1}^{N} K_i \tag{10}$$

where K_i is the elemental stiffness matrix, and N is the total number of elements of the discrete structure in Figure 4.

4 Numerical Analysis

In this section, a domestic oil well is taken to study the stress field of the CCF multilayer composite system, the structural diagram is shown in Figure 5(a). According to the basic principle of elastic mechanics, the mechanical problem of CCF multilayer composite system is the axisymmetric strain in the plane. Therefore, a quarter of the model is modeled to analyze the stress distribution. The FEM meshing model is shown in Figure 5(b). The inner walls between casings, cement sheathes and formation are all set to be welded. The minimum horizontal in-situ stress is applied to the upper boundary of the model; the maximum horizontal in-situ stress is applied to the right boundary; the normal displacement constraint is applied to the bottom and left boundary of the model, respectively.

The geometric and material parameters are listed in Table 2; the maximum of horizontal in-situ stress is 20 MPa; the minimum of horizontal in-situ stress is 13 MPa; the pressure of drilling fluid p_w is 30 MPa;

Table 2 Geometric and material parameters of casing-cement-formation multilayer composite system, where the r_{inner} represents the inner radius

Material	r_{inner}/mm	E/ GPa	μ
Casing-1	162.5	210	0.21
Cement sheath-1	178.3	8.5	0.3
Casing-2	229.1	210	0.21
Cement sheath-2	248.0	8.5	0.3
Formation	298.5	3.1	0.25

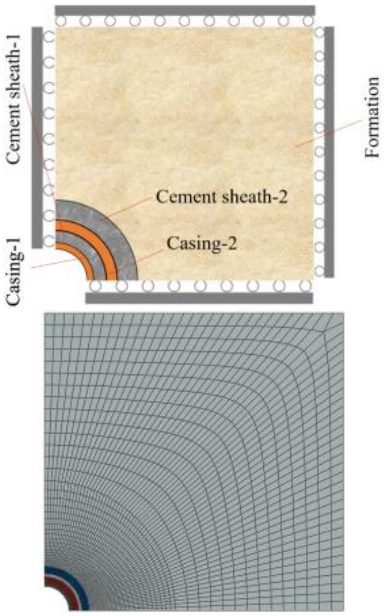

Figure 5 Physical model (a) and meshing (b) of casing-cement-formation multilayer composite system

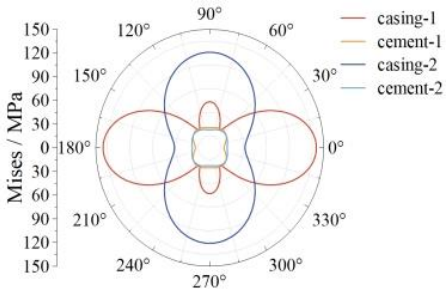

Figure 6 Mises stress distribution on the inner walls of multilayer composite

Figure 6 shows the mises distribution on the inner walls of casing-1, cement sheath-1, casing2 and cement sheath-2. It can be seen that the mises stress of casing-1 is larger than cement-1, and the mises stress of casing-2 is also larger than cement-2. This is because the elastic modulus of the casing is much larger than cement sheath. In addition, the mises stress distribution on the inner walls of casings and cements are non-uniform, which is caused by the deviatoric in-situ stress mentioned in Eq. 1. The above results are consistent in the mechanical analysis in section2, which verifies the numerical model of the CCF multilayer composite system.

Figure 7 Physical model of casing-cement-formation single composite system

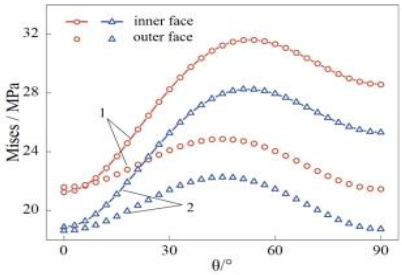

Figure 8 Mises stress distribution of inner and outer walls of cement sheathes, where 1 denote the cement sheath-1 in casing-cement-formation single composite system, and 2 denote the cement sheath in multilayer composite system

Based on the values listed in Tab. 2, we also calculated a single layer CCF system without casing 2 and cement sheath 2, as shown in Figure 7. The mises stress distribution of cement sheathes in multilayer composite system and single layer composite system were plotted in Figure 8. Figure 8 indicates that the mises stress of cement sheath in multilayer composite system is apparently significantly small than that in single composite system. Compared to the single composite system, the mises stress on the inner wall of cement sheath in multilayer composite system is decreased by 3.4MPa, and 7MPa decreased on the outer wall. Therefore, it is easy to find that the multilayer composite system can effectively enhance the stability of the wellbore.

In the rest of words, the sensitivity analysis of main influence mechanical parameters such as in-situ stress, the elastic of cement sheathes and the elastic of formation are conducted. Given the limited space, the cement sheathes shown in Figure 5(a), which is the most important and easily damaged in CCF system, is taken as the main study object.

4.1 Elastic modulus of formation

To investigate the effect of elastic modulus of formation, a range of sensitivity analysis conducted under the identical in-situ stress and modeling conditions. Figure 9 and Figure 10 shows the inner wall mises stress distribution of cement sheath-1 and cement sheath-2, respectively, for the values of elastic modulus of formation as 5GPa, 10GPa, 15GPa, 20GPa and 25GPa; Figure 10 presents the simulation results of the maximum mises stress versus the elastic modulus of formation.

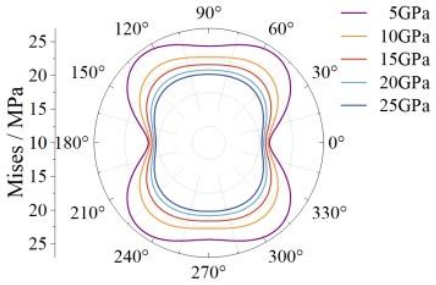

Figure 9 Mises stress distribution of cement sheath-1 inner wall under different elastic modulus of formation

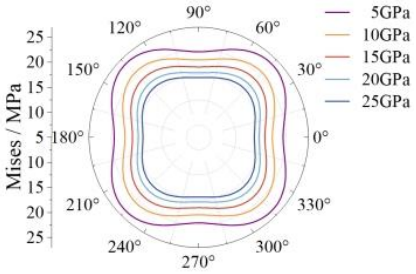

Figure 10 Mises stress distribution of cement sheath-2 inner wall under different elastic modulus of formation

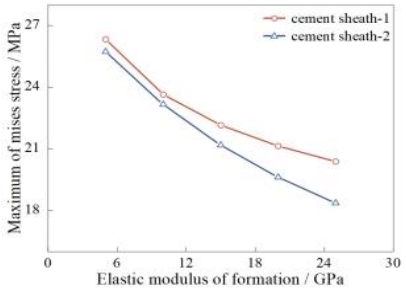

Figure 11 The variation of the maximum Mises stress on cement sheathes with different formation elastic modulus

As revealed from the results, with the elastic modulus of formation varying from 5GPa to 25GPa, the mises stress in the cement sheath-1 and 2 decreases, which indicates that the multilayer composite system is endurable in the formation of high elastic modulus. The maximum mises stress of cement sheath-1 is greater than that of cement sheath-2 under the identical elastic modulus of formation. The slope of the maximum mises stress curve of cement sheath-2 is larger than that of cement sheath-1, which demonstrates that the cement sheath-2 is more sensitivity to the differences of the elastic modulus of formation. Based on the above, it is advised that the CCF multilayer composite system is more suitable for stratum with high elastic modulus.

4.2 In-situ stress

In order to demonstrate the effects of the in-situ stress on the stress distribution of CCF multilayer composite system, several numerical simulations under different in-situ stress are conducted. Under the constant in-situ stress ratio $\sigma_h / \sigma_H = 0.7$, calculations are developed

with several value sets of maximum horizontal and vertical in-situ stress listed in Tab. 3. Figure 12 and Figure 13 show the inner wall mises stress distribution of cement sheath-1 and cement sheath-2, respectively; Figure 14 illustra;5tes the simulation results of the maximum mises stress versus the in-situ stress.

According to the results form Figure 12 and 13, with the σ_h is altered form 3MPa to 15MPa, the mises stress in the cement sheath-1 and 2 increases. In Figure 14, the slope of the maximum mises stress curve of cement sheath-2 is larger than that of cement sheath-1, which indicates that the cement sheath-2 is more sensitivity to the differences of the in-situ stress under the constant in-situ stress ratio σ_h / σ_H = 0.7. Additionally, when σ_h varying from 3MPa to 15MPa, the maximum mises stress of cement sheath-1 is greater than that of cement sheath-2, and the difference between these tends to close as the σ_h increases. Based on the above, it is advised that more attention should be paid to the design of cement sheath-2 strength when the value of in-situ stress is too high.

Table 3 In-situ stress of formation, where σ_H is the maximum horizontal in-situ stress, σ_h is the maximum vertical in-situ stress

Number	σ_H / MPa	σ_h / MPa
1	4.3	3
2	8.6	6
3	12.9	9
4	17.1	12
5	21.4	15

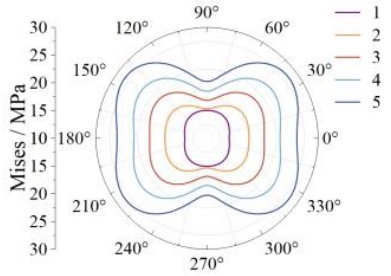

Figure 12 Mises stress distribution of cement sheath-1 inner wall under different in-situ stress, where 1, 2, 3,4 and 5 represent the in-situ set number in Table 3

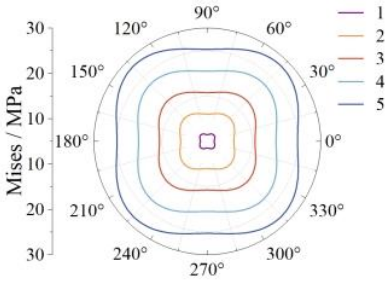

Figure 13 Mises stress distribution of cement sheath-2 inner wall under different in-situ stress, where 1, 2, 3,4 and 5 represent the in-situ set number in Table 3

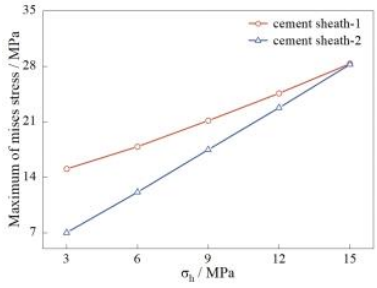

Figure 14 The variation of the maximum Mises stress on cement sheathes under different formation in-situ stress listed in Table 3

4.3 Elastic modulus of cement sheath

For the CCF multilayer composite system, the mechanical parameter of material is one of keys to the mechanical performance. Actually, the mechanical properties of casing are generally constants in engineering, and the main difference between various cement sheath is elastic modulus. Therefore, the effect of elastic modulus of cement sheath on the multilayer composite system is mainly discussed in this section. A series of numerical simulations with different elastic modulus of cement sheath-1 and cement sheath-2 are conducted, respectively.

4.3.1 Cement sheath-1

Figure 15 and Figure 16 show the inner wall mises stress distribution of cement sheath-1 and cement sheath-2 when the elastic modulus of cement formation-1 is 5GPa, 25 GPa, 45 GPa and 65 GPa, respectively. Figure 17 exhibits the maximum mises stress versus the elastic modulus of cement sheath-1.

Figure 15 shows that the inner wall mises stress of cement sheath-1 decreases with the increase of elastic modulus of cement sheath-1. According to the Figure 16, when the elastic modulus of cement sheath-1 increases, the values of mises stress decreases in the well angle is 45 ° to 135 °, and increases in the well angle is 135 ° to 225 °. Meanwhile, the maximum value of cement sheath-2 stays around 27Mpa. Figure 17 presents the simulation results of the maximum mises stress versus the elastic modulus of cement sheath-1, it is noticeably observed that the maximum mises stress of cement sheath-1 is much more sensitive than that of cement sheath-2.

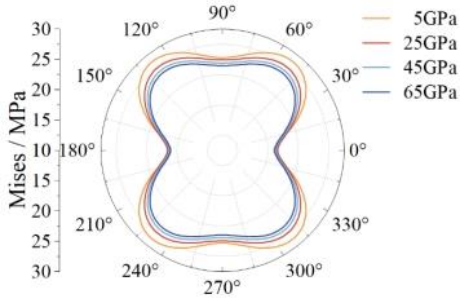

Figure 15 Mises stress distribution of cement sheath-1 inner wall under different elastic modulus of cement sheath-1

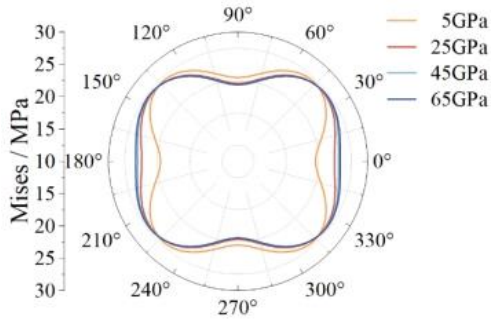

Figure 16 Mises stress distribution of cement sheath-2 inner wall under different elastic modulus of cement sheath-1

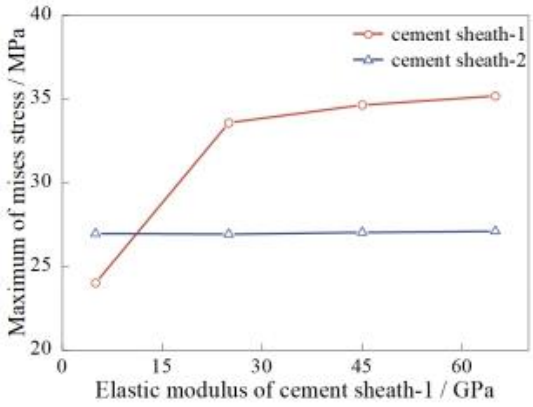

Figure 17 The variation of the maximum mises stress on cement sheathes under different elastic modulus of cement sheath-1

4.3.2 Cement sheath-2

Figure 18 and Figure 19 shows the inner wall mises stress distribution of cement sheath-1 and cement sheath-2 when the elastic modulus of cement formation-2 is 5GPa, 25 GPa, 45 GPa and 65 GPa, respectively. Figure 20 exhibits the maximum mises stress versus the elastic modulus of cement sheath-2.

As revealed form the results, the maximum mises stress of cement sheath-1 decreases with the increase of the elastic modulus of cement sheath-2. On the contrary, the maximum mises stress of cement sheath-2 increases with the increase of the elastic modulus of cement sheath-2.

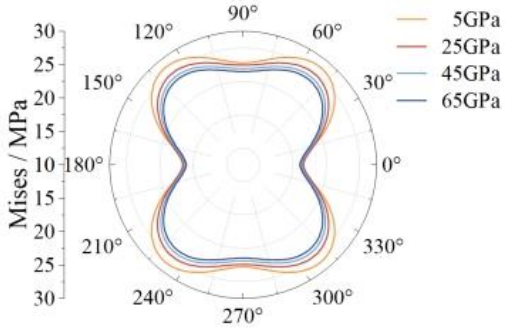

Figure 18 Mises stress distribution of cement sheath-1 inner wall under different elastic modulus of cement sheath-2

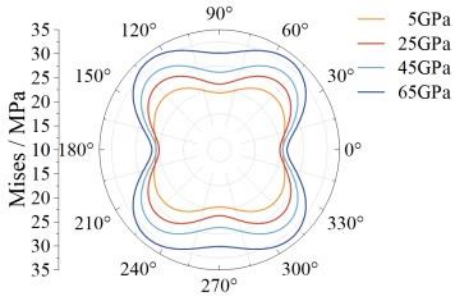

Figure 19 Mises stress distribution of cement sheath-2 inner wall under different elastic modulus of cement sheath-2

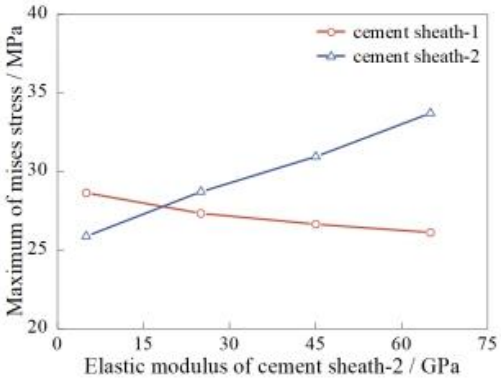

Figure 20 The variation of the maximum Mises stress on cement sheathes under different elastic modulus of cement sheath-2

Based on the comprehensive analysis of the elastic modulus of two cement sheathes, some suggestions are supposed that the elastic modulus of cement sheath-1 should be set around 5GPa and the elastic modulus of cement sheath-2 should be set around 5GPa to 30GPa. This setting could effectively improve the stability of the CCF multilayer composite system.

5. Conclusion

The theoretical analysis of casing-cement-formation multilayer composite system is elaborated. The FEM model of CCF multilayer composite system is constructed and a series of numerical simulations are conducted. Results indicate that the CCF multilayer composite system possesses better performance than the CCF system with single casing and cement sheath. Meanwhile, the sensitivity analysis which is the main influence of mechanical parameters of cement sheathes and formation is conducted.

In the inner wall of cement sheath-1 and cement sheath-2, the mises stress decreases as the elastic modulus of formation varying from 5GPa to 25GPa; and the mises stress increases as the in-situ stress increases, and the cement sheath-2 is more sensitivity to the in-situ stress under the constant in-situ stress ratio σ_h / σ_H = 0.7. Furthermore, the elastic modulus of cement sheath is essential for the stress distribution, in this paper, the

proper values of elastic modulus of cement sheath-1 and cement sheath-2 are 5GPa and 5GPa to 30GPa, respectively. This research can be helpful to design the structure of CCF multilayer composite system.

Conflict of Interest: We are committed to that there is no conflict of interest regarding the publication of this paper.

Acknowledgments: The authors of this paper acknowledge the supports from the Independent Innovation Research Program of China University of Petroleum (East China) (Grant No. 27RA2215005) and the National Key Research and Development Program of China (Grant No. 2017YFC0307604).

This is the Appendix: This article does not cover the details that require an appendix.

References

[1] De Simone Marcelo, Pereira Fernanda L.G. and Deane Mesquita Roehl. Analytical methodology for wellbore integrity assessment considering casing-cement-formation interaction [J]. International Journal of Rock Mechanics and Mining Sciences, 2016, 94: 112-122.

[2] Wei Liu, Baohua Yu, and Jingen Deng. Analytical method for evaluating stress field in casing-cement-formation system of oil/gas wells [J]. Applied Mathematics and Mechanics, 2017, 38(9): 1273-1294.

[3] Yang Heng, Bu Yuhuan, Guo Shenglai, et al.. Effects of in-situ stress and elastic parameters of cement sheath in salt rock formation of underground gas storage on seal integrity of cement sheath [J]. Engineering Failure Analysis, 2021, 123: 105258.

[4] Guo Xinyang, Bu Yuhuan, Li Juan, et al.. Modes and prevention of cement sheath failures under complex downhole conditions [J]. Nature Gas Industry, 2013, 33(11): 86-91.

[5] Qu Zhan, Wang Xiaozeng and Dou Yihua. Analytic and Numerical Solutions of Load and Stress of Casing and Cement in Cementing Section [J]. Applied Mechanics and Materials, 2012, 268-270(268-270): 721-724.

[6] Yin Youquan, Chen Chaowei, Li Pingen. Theoretical solutions of stress distribution in casing-cement and stratum system [J]. Chinese Journal of Theoretical and Applied Mechanics, 2006, 28(6): 835-842.

[7] Yin Youquan, Cai Yongen, Chen Chaowei, et al.. Theoretical solution of casing loading in non-uniform ground stress field [J]. Acta Petrolei Sinica, 2006, 27(4): 133-138.

[8] Zhang Hong, Shen Ruichen, Li Jingcui, et al.. Elastoplastic Analysis of Cement Sheath of Injection Production Wellbore Under Varied Casing Pressure [J]. Arabian Journal for Science and Engineering, 2018, 43(11): 6523-6534.

[9] Wang Hongwei, Fang Xinding, Zhang Shuangxi, et al.. An analytical approach for cased borehole stress calculation in general anisotropic formations [J]. International Journal for Numerical and Analytical Methods in Geomechanics, 2021, 45(1): 3-27.

[10] Wang Hongwei, Miao Miao, Zhou Tao et al.. An analytical approach to the stress distribution around a cased borehole in an anisotropic formation [J]. Applied Mathematical Modelling, 2022, 107: 316-331.

[11] Yu Guimin, Xu Jie, Liu Wei, et al.. A Modified Model of Cement Sheath Stress Distribution with a Fixed Far-Field Displacement Boundary Condition [J]. Chemistry and Technology of Fuels and Oils, 2023, 59(2): 362-374.

[12] Zhou Bo, Zhang Chao, Zhang Xudong, et al.. A semi-analytical method for the stress distribution around a borehole with multiple casings and cement sheaths [J]. Geoenergy Science and Engineering, 2023, 229: 212091.

[13] Kuanhai Deng, Yue Yuan, Yi Hao, et al.. Experimental study on the integrity of casing-cement sheath in shale gas wells under pressure and temperature cycle loading [J]. Journal of Petroleum Science and Engineering, 2020, 195: 107548.

[14] Dou Haoyu, Dong Xuelin, Duan Zhiyin, et al.. Cement Integrity Loss due to Interfacial Debonding and Radial Cracking during COsub2/sub Injection [J]. Energies 2020, 13(17): 4589-4589.

[15] Maryam Tabatabaei, Arash Dahi Taleghani and Nasim Alem. Measurement of mixed mode interfacial strengths with cementitious materials [J]. Engineering Fracture Mechanics, 2020, 223: 106739.

[16] Bu Yuhuan, Tian Leiju, Guo Bingliang, et al.. Experiment and simulation on the integrity of cement ring interface in deep water shallow formation [J]. Journal of Petroleum Science and Engineering, 2020, 190: 107127-107127.

[17] Wu Yuxing, Harshkumar Patel, Saeed Salehi, et al.. Experimental and finite element modelling evaluation of cement integrity under diametric compression [J]. Journal of Petroleum Science and Engineering, 2020, 188: 106844-106844.

[18] Li Juan, Guo Xinyang, Bu Yuhuan, et al.. Investigation on preventing mechanical failure of cement sheath in fractured wells by expanding cement [J]. Oil Drilling & Production Technology, 2014, 36(4): 43-46.

[19] Yan yan, Guan Zhichuan, Wang qing, et al.. Experiment on damage of cement sheath induced by perforation in oil and gas wells [J]. Journal of China University of Petroleum. 2022, 46(3): 81-88.

[20] Kubacka Ewelina and Ostrowski Piotr. Heat conduction issue in biperiodic composite using Finite Difference Method [J]. Composite Structures, 2021, 261: 113310.

[21] Ma xiao and Wei Gaofeng. Numerical prediction of effective electro-elastic properties of three-dimensional braided piezoelectric ceramic composites [J]. Composite Structures, 2017, 180: 420-428.

[22] Zhou Bo, Kang Zetian, Wang Zhiyong, et al.. Finite element method on shape memory alloy structure and its applications. Chinese Journal of Mechanical Engineering, 2019, 32(84): 1-11.

[23] Sun Fenglong, Gong yanpeng and Dong Chunying. A novel fast direct solver for 3D elastic inclusion problems with the isogeometric boundary element method [J]. Journal of Computational and Applied Mathematics, 2020, 377: 112904.

[24] Ma Xiao, Zhou Bo and Xue Shifeng. A meshless Hermite weighted least-square method for piezoelectric structures[J]. Applied Mathematics and Computation, 2021, 400:1-15.

[25] Deng Hu and Jia Lichun. Key technologies for drilling deep

and ultra-deep wells in the Sichuan Basin: Current status, challenges and prospects [J]. Natural Gas Industry, 2022, 42(12): 82-94.

[26] Chang Deyu, Li Gensheng, Shen Zhonghou, et al.. The stress field of bottom hole in deep and ultra-deep wells [J]. Acta Petrolei Sinica, 2011, 32(4): 697-703.

[27] Wu Yi, Zhou Jianliang, Yang Jin, et al.. A Study on the Integrity Evaluation of Cement Sheaths for Deep Wells in Deep Water [J]. Energies, 2022, 15(16),5814-5814.

[28] Ding Shidong, Liu Kui, Liu Xiaogang, et al.. The Effect of Pre-Applied Annulus Back Pressure Cementing on Radial Stress of Interfaces in Double Layer Casing Systems [J]. Petroleum Drilling Techniques, 2022, 50(1): 30-37.

[29] Zhao Xinbo, Han Shengchao, Yang Xiujuan, et al.. Mechanical characteristics analysis of casing-cement sheath-formation multilayer composite system with thermo-structural coupling effects, 2017, 48(3): 837-843.

[30] Zhou Bo, Xue Shifeng and Zhu xiuxing. Solid Mechanics: Theory and MATLAB Solution [M]. Press of China University of Petroleum, Beijing China, pp. 49–70.

[31] Wang Yanbin, Gao Deli, Fang Jun. Mechanical characteristics analysis of casing-cement ring-formation multilayer composite system [J]. Chinese Journal of Applied Mechanics, 2014, 21(3): 387-392.

[32] Zhou Bo, Zhang Chao and Zhao Fei. A Finite Element-Meshless Hybrid Method (FEMLHM) of Elasticity Problem and Its Applications [J]. Mechanics of Solids, 2023, 58(3): 852-871.

[33] Li Yong, Ji Hongfei, Xing Pengju, et al.. Theoretical solutions of temperature field and thermal stress field in wellbore of a gas well [J]. Acta Petrolei Sinica, 2021, 42(1): 84-94.

[34] Huang Zhongwei, Li Gensheng, Wang Yongzhang, et al.. Hydra-jet fracturing applied in a well with three-layer casings [J]. Oil Drilling & Production Technology, 2012, 34(5): 122-124.